Experimental characterisation of the reactive properties of premixed ammonia flames

Alka Karan, Guillaume Dayma, Christian Chauveau, Fabien Halter

Experimental characterisation of the reactive properties of premixed ammonia flames

Alka Karan[1,2], Guillaume Dayma[1,2], Christian Chauveau[1], Fabien Halter[1,2]
[1]ICARE-CNRS
1C Avenue de la Recherche Scientifique, 45071 Orléans Cedex 2, France
[2]Université d'Orléans
Chateau de la Source, 45100 Orléans, France

ABSTRACT

Ammonia is promoted as a potential alternative fuel due to its no carbon emissions. Obtaining laminar flame speed at high pressure and temperature for near stoichiometric conditions is important for engine sizing. A wide range of experimental conditions have been explored along with the evaluation of the most recent kinetic mechanisms. It is also interesting to study the inner structure of the premixed ammonia flame at standard conditions to understand the combustion process and to precisely determine the flame speed. For thick flames, the isotherm selection plays a major role.

1. Introduction

The need for environment friendly energy resources have led to a deep research in non-carbon fuels like ammonia and hydrogen. It is important to study various properties of the fuel to characterize its performance. One such important parameter is the laminar flame speed which is a sizing parameter for industrial systems. It is required to have laminar flame speed data at the working conditions of engines i.e. at high pressure and temperature for near stoichiometric conditions. A wide range of data can help to have an empirical relation to find flame speed for any pressure and temperature for a given set of initial conditions. The previous work reported laminar flame speeds for a maximum temperature and pressure of 485 K and 20 bar [1]. The present work aims to extend these limits to 585 K and almost 30 bar and to provide a general correlation for this large range of experimental conditions. The most recent kinetic mechanisms existing in the literature have been chosen and evaluated for the same conditions. Furthermore, it is interesting to study the inner structure of the flame to understand how the combustion process can be enhanced for a better performance. It is known that ammonia flames are thick [2]. When the characteristic flame thickness is more than 1 mm, there is a need to precisely define the isotherm associated to fresh gases side as the flame speed evaluation is highly dependent on it.

2. Method

2.1 Experimental set up

The most common methods to determine the laminar flame speed experimentally include closed spherical constant pressure chamber, stagnation/counterflow method, heat flux burner, Bunsen burner, and externally heated channel. However, the most accurate method of measuring the flame speeds for a large range of extreme conditions is the constant volume spherically outward propagating flame. The experiments are performed in the OPTIPRIME facility of ICARE-CNRS, Orléans, France and has been described in [3].

In order to study the inner structure of the flame, a Bunsen burner along with a co-flow of stoichiometric methane-air flame is used. The pilot flame does not influence the main flame as the power emitted by the pilot flame is less compared to the power emitted by the main flame which is in between 83 and 117 W. The mean velocity of the fresh gases at the exit of the burner ranged from 0.18 to 0.2 m/s. The flame speed was determined using a PIV set-up. The airflow is fed through a seeding system, consisting of an atomizer that produces droplets of size 1 µm. Di-ethyl-hexyl-sebacate (DEHS) which evaporates at 525 K was used to seed the fresh gases with droplets. The PIV set-up consists of a laser source directed to a dichroic mirror kept at 45°. The light source used is a continuous Coherent Verdi G20 Laser of 532 nm. A laser power of 5 W is used. The light from this source is reflected at the mirror at a right angle penetrating through a spherical lens of a focal length, f=750 mm which further goes through a cylindrical lens providing a laser sheet perpendicular to the flame. An iris is used to control the size of the laser sheet projected on the burner to ensure that only the flame is illuminated by the laser. A CMOS camera (PHANTOM V1611) is used to capture the images and a code written in Python is used to track the particles and provide a velocity field map. A PIV interrogation window size of 32 pix^2 is set initially. Finally, an interrogation window size of 16 pix^2 with a 50% overlap is used. The magnification factor is 4.56E-2 mm/pix and the camera acquisition rate and the exposure time were set to 100 fps and 3000 µs respectively. Fig. 1 represents the schematic diagram of the set-up.

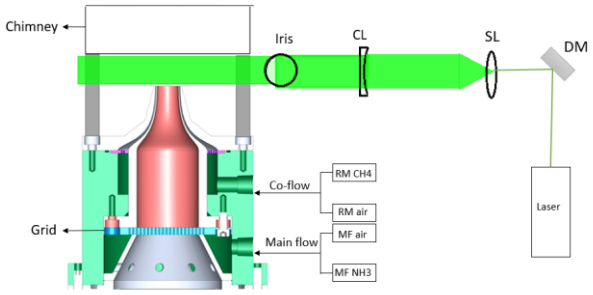

Fig. 1: Schematic diagram of the experimental set-up along with the PIV set-up. CL: cylindrical lens, SL: spherical lens, DM: dichroic mirror, RM: rotameter, MF: mass flowmeter.

Corresponding author: Fabien Halter
E-mail address: fabien.halter@cnrs-orleans.fr

Table 1 Initial conditions for the experiments performed. The initial temperature, T_0, was maintained at 300 K and the oxidizer consisted of 30% O_2 and 70% diluent.

φ	P_0(bar)	Diluent
0.8	1	49 % Ar 21 % He
0.8	2	49 % Ar 21 % He
1.1	1	49 % Ar 21 % He
1.1	2	49 % Ar 21 % He
1.1	1	21 % Ar 49 % He
1.1	2	21 % Ar 49 % He
1.1	3	49 % Ar 21 % He
1.1	4	70 % He
1.3	1	21 % Ar 49 % He
1.3	2	21 % Ar 49 % He
1.3	2	21 % Ar 49 % He
1.3	3	21 % Ar 49 % He
1.3	4	21 % Ar 49 % He
1.3	4	70 % He

2.2 Experimental conditions and measurement of flame speeds

The experimental conditions investigated in the constant volume spherical chamber are presented in Table 1. The oxy-ammonia flames are quite unstable as both hydrodynamic and thermo-diffusive instabilities are favored at high temperatures and pressures and so diluents are used to stabilize the flame conditions. The flame speeds were calculated with the given radius and pressure using the given equation [3]:

$$S_u = \frac{dR_f}{dt} - \frac{\left(R_0^3 - R_f^3\right)}{3\,\gamma_u R_f^2 P}\frac{dP}{dt} \quad (1)$$

where R_f and R_0 are the flame radius and the inner chamber radius respectively and γ_u is the heat capacity ratio of the unburnt gases.

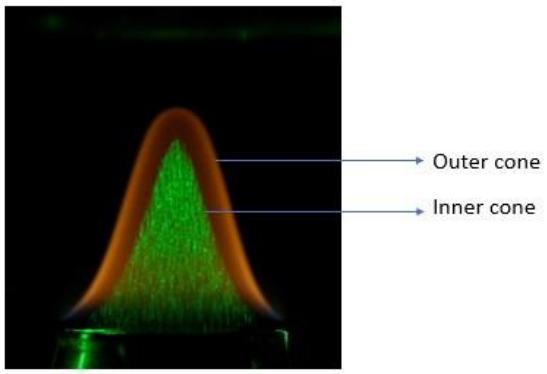

Fig. 2 Ammonia-air flame at φ= 1.1 with PIV depicting the thick flame. The inner cone and the outer cone represent the fresh gas surface and the outer flame surface respectively. The camera used to capture this image is NIKON D850 and the exposure time has been set to 250 s

For the case of the Bunsen burner, the experimental conditions range for an equivalence ratio between 1 and 1.4 as stable flames were obtained for these conditions. The laminar flame speeds were calculated by determining the right isotherm and applying the mass continuity equation. As shown in Fig. 2, it is seen that the inner cone corresponding to the fresh gas surface and the outer cone corresponding to the outermost visible flame surface cannot be approximated to a single isotherm due to the thickness of the flame. Hence, the surface area of the fresh gases and the burnt gases cannot be equal while considering the mass continuity equation which is given as follows:

$$A_b U_{fg} = A_u S_L \quad (2)$$

where U_{fg} is the fresh gases velocity at the burner outlet, A_b is the exit area of the burner and A_u is the area of the unburnt gas surface.

The displacement speed, S_d is dependent on the chosen iso-surface and is given as:

$$S_d = (u - w).n \quad (3)$$

where u is the fluid velocity, w is the absolute speed of the flame in a fixed laboratory frame and n is the flame normal vector oriented towards the fresh gases. Here, w=0.

2.3 Chemical kinetic mechanisms

A literature review was performed to select 9 of the most recent kinetic mechanisms for ammonia combustion. The simulations were performed using the premixed laminar flame speed calculator available in Chemkin-*Pro* to obtain the laminar flame speeds for the experimental conditions given in Table 1. Sensitivity analyses were performed to identify the key reactions influencing the flame speed in these mechanisms.

3. Results and Discussion

Fig. 3 represents the flame speeds at ϕ = 1.1, diluent mixture of 49% He and 21% Ar, T_0 = 300 K, p_0 = 1, 2, and 3 bar as a function of *P* and *T*. The experimental data are the blue, red, and green thick lines in the volume. The blue, red, and green thin lines on the lower plane are the projections of these experimental data on the (*P*, T) plane representing the isentropic evolution of pressure and temperature starting from each initial condition. The S_L = f (*P, T*) map is generated by using the equation (3) proposed by [4] to fit the experimental results under these conditions.

$$S_u = S_{u0}\left(\frac{T}{T_0}\right)^{xT+y}\left(\frac{p}{p_0}\right)^{a\exp\left(\frac{-p}{b}\right)+c} \quad (3)$$

Under the conditions of Fig. 3, the experimental data are best reproduced using $x = 1.65\times10^{-3}$, $y = 1.673$, $a = 0.742$, $b = 0.112$, $c = -0.171$.

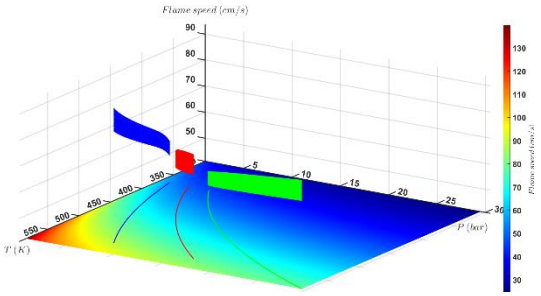

Fig. 3: Experimental flame speeds of $NH_3/O_2/He/Ar$ mixtures at φ = 1.1, T_0 = 300 K, p_0 = 1 (blue), 2 (red), and 3 bar (green).

As illustrated by the Fig. 4, on analyzing all the cases, it was concluded that both Nakamura [5] and Stagni [6] mechanisms can predict the flame speed closest to the experimental values, that from Nakamura [5] being more difficult to converge.

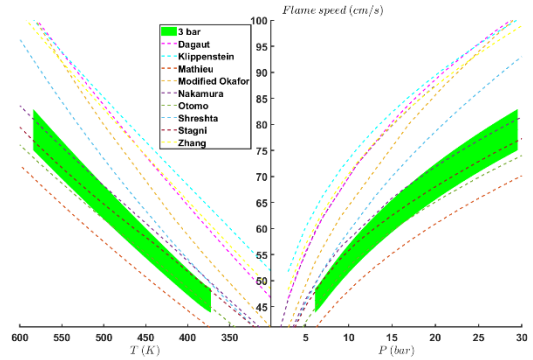

Fig. 4: Comparison of experimental flame speeds of $NH_3/O_2/He/Ar$ mixtures at φ = 1.1, T_0 = 300 K, p_0 = 3 bar with different kinetic mechanisms.

Now switching to the Bunsen burner configuration, the green isotherm (Fig. 2) of the inner cone is the 525 K isotherm where the DEHS droplets evaporate. The orange colour is the characteristic chemiluminescence of NH_2 radicals produced in the flame zone. The flame thickness, δ, is defined as the zone between the inner and outer cone. As per the definition of the flame speed, the isotherm to be chosen corresponds to the fresh gases surface. The laminar flame speed, S_L, and the displacement speed, S_d are computed using equations 2 and 3 respectively. The difference in the flame speed computed at the outer cone (OC) and the inner cone (IC) represented by black square and dash respectively in Fig. 5 is around 2-3 cms^{-1}. On comparing with values given in the literature, it is seen that the flame speeds reported in the literature are closer to the flame speed obtained at the outer cone as shown in Fig. 5. It can also be seen that the displacement speed evaluated at the inner cone which is represented by the black diamond in Fig. 5 is in congruence with the laminar flame speed at the same surface.

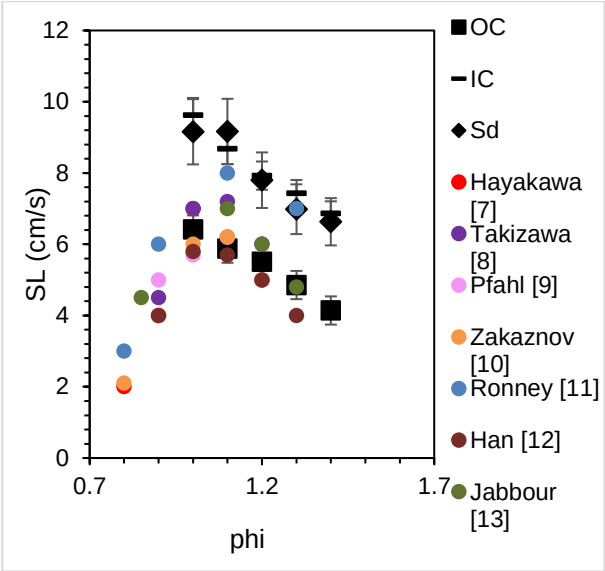

Fig. 5: Comparison of ammonia-air laminar flame speed at atmospheric conditions available in the literature for different φ. OC (black square) and IC (black dash) represent the flame speed at the outer cone and inner cone and Sd represented by black diamond is the displacement flame speed.

4. Concluding Remarks

Experiments to measure flame speeds of ammonia at elevated conditions of pressure and temperature corresponding to those encountered in spark-ignition engines and gas turbines have been performed. The test conditions range over an initial pressure of 1 to 4 bar, at an initial temperature of 300 K for three different equivalence ratios: 0.8, 1.1 and 1.3. The experiments provide flame speed data for a pressure of almost 30 bar and a temperature of 585 K. Amongst the most recent kinetic mechanisms, it was seen that both Nakamura [5] and Stagni [6] predicted flame speeds close to the experimental values for all conditions. In order to understand the combustion process, a conical flame at standard conditions was studied. It was seen that the thickness of the ammonia/air mixtures is quite important and thin flame approximation cannot be applied. To remain in consistency with the theoretical definition of the flame speed, the iso-surface corresponding to the fresh gases needs to be chosen. The laminar flame speed for ammonia-air flame at atmospheric conditions for equivalence ratios, φ= 1-1.4 has been evaluated by choosing the isotherm as per the definition.

References

[1] Karan A, Dayma G, Chauveau C, Halter F, *ICFD,* 17, (2020).

[2] Kobayashi H, Hayakawa A, Somarathne KDKA, Okafor EC. Science and technology of ammonia combustion, *Proc. Combust. Inst.,* 37, (2019), 109-133.

[3] Halter F, Dayma G, Serinyel Z, Dagaut P, Chauveau C. Laminar flame speed determination at high pressure and temperature conditions for kinetic

schemes assessment, *Proc. Combust. Inst., 38, (2021), 2449-2457.*
[4] Hu E, Li X, Meng X, Chen Y, Cheng Y, Xie Y, Huang Z. Laminar flame speeds and ignition delay times of methane-air mixtures at elevated temperatures and pressures, *Fuel.,* 158, (2015), 1-10.
[5] Nakamura H, Hasegawa S. Combustion and ignition characteristics of ammonia/air mixtures in a micro flow reactor with a controlled temperature profile, *Proc. Combust. Inst.,* 36, (2017), 4217-4226.
[6] Stagni A, Cavallotti C, Arunthanayothin S, Song Y, Herbinet O, Battin-Leclerc F, Faravelli T. An experimental, theoretical and kinetic-modeling study of the gas-phase oxidation of ammonia, *Reac. Chem. Eng.,* 5, (2020), 696-711.
[7] Hayakawa A, Goto T, Mimoto R, Arakawa Y, Kudo T, Kobayashi H. Laminar burning velocity and markstein length of ammonia/air premixed flames at various pressures, *Fuel.,* 159, (2015), 98-106.
[8] Takizawa K, Takahashi A, Tokuhashi K, Kondo S, Sekiya A. Burning velocity measurements of nitrogen-containing compounds, *J. Hazard. Mater.,* 155, (2008), 144-152.
[9] Pfahl UJ, Ross MC, Shepherd JE, Pasamehmetoglu KO, Unal C. Flammability limits, ignition energy and flame speeds in H_2-CH_4-NH_3-N_2O-O_2-N_2 mixtures, *Combust. Flame,* 123, (2000), 140-158.
[10] Zakaznov VF, Kursheva LA, Fedina ZI. Determination of normal flame velocity and critical diameter of flame extinction in ammonia-air mixture, *Combust. Explos. Shock Waves,* 14, (1978), 710-713.
[11] Ronney PD. Effect of chemistry and transport properties in near-limit flames at microgravity, *Combust. Sci. Technol.,* 59, (1988), 123-141.
[12] Han X, Wang Z, Costa M, Sun Z, He Y, Cen K. Experimental and kinetic modeling study of laminar burning velocities of NH_3/air, NH_3/H_2/air, NH_3/CO/air and NH_3/CH_4/air premixed flames, *Combust. Flame,* 206, (2019), 214-226.
[13] Jabbour T, Clodic DF. Burning velocity and refrigerant flammability classification, *Trans. – Am Soc. Heat Refrig. Air Cond. Eng.,* 110, (2004), 522-533.